Energy Reports 4 (2018) 31–40

Contents lists available at ScienceDirect

Energy Reports

journal homepage: www.elsevier.com/locate/egyr

Research paper

Evaluation of durability of composite materials applied to renewable marine energy: Case of ducted tidal turbine

M. Nachtane [a,b,*], M. Tarfaoui [a], D. Saifaoui [b], A. El Moumen [a], O.H. Hassoon [c], H. Benyahia [a]

[a] ENSTA Bretagne, FRE CNRS 3744, IRDL, F-29200 Brest, France
[b] Laboratory for Renewable Energy and Dynamic Systems, FSAC - UH2C, Morocco
[c] University of technology, Iraq

ARTICLE INFO

Article history:
Received 22 September 2017
Received in revised form 30 December 2017
Accepted 4 January 2018

Keywords:
Marine composite structures
Ducted tidal turbine
Finite element analysis
VUMAT

ABSTRACT

Composite materials are used in many marine structures such as renewable marine energy conversion systems because of their fairly good mechanical properties and especially their low densities compared to traditional materials. The most advanced features currently available in finite element (FE) Abaqus/Explicit have been employed to simulate the behavior of the composite nozzle under hydrodynamic and impact loading. A hydrodynamic analysis was considered to design the nozzle turbine and the hydrodynamic pressure obtained was then implemented as boundary conditions to a FE code. The goal of this article is to evaluate the durability of composite materials of a ducted tidal turbine under critical loads (hydrodynamic and hydrostatic pressures) with the implementation of a failure criterion using the finite element analysis (FEA). The mechanical behavior was analyzed for two materials (Carbon–epoxy/Glass–polyester). This has been accomplished by forming a user-created routine (VUMAT) and executing it in the ABAQUS software.

1. Introduction

Growing concern over the threat of global climate change has led to an increased interest in research and development of renewable energy technologies. Marine renewable energies can contribute to the diversification of the global energy mix because they have the advantage of providing a modular production (Mourad et al., 2018). In this context, composite materials will play a key role in this emerging industry because they have specific mechanical properties that are very remarkable in terms of reliability and durability (Smith, 1990). And because of its good experience in the marine environment and applications such as wind turbines and tidal turbines where they are subject to critical loads, very little information is available on their behavior in the water. However, the major disadvantage of using these materials is the mastery of the evolution of its mechanical properties due to the complexity of mechanisms of mechanical and environmental damage (temperature, pressure, humidity, etc.) which can create irreversible degradation preventing the performance specifications from being met (Davies and Lemoine, 1992). It is therefore essential to control the evolution of the properties of the material during its operation, in order to predict the lifetime of the composites.

Today, marine energy conversation systems such as marine current turbine that use the composite material that is currently the best way to achieve a balance between performance, weight and structural integrity because the marine environment is particularly demanding and aggressive: Salt corrosion, the forces of currents and storms (Boisseau et al., 2013). The advantage of glass reinforced polymer (GFRP) composites is that they are relatively inexpensive and offer sufficient strength and stiffness. The size of the turbines increases; the carbon fiber reinforced polymer (CFRP) becomes more popular for the development of certain parts such as blades and nozzle (Boisseau et al., 2012). Carbon fibers normally cost 10 to 20 times more than fiberglass. In fact, carbon fibers provide a much higher modulus and a significant weight reduction (Nachtane et al., 2016).

Tidal currents can provide a significant and predictable source of renewable energy. This work will research the use of composite materials for the nozzle of a tidal turbine to harness this energy. The rotor blades are currently made of steel, which leads to several problems in the marine environment, expensive manufacturing processes and difficulties in handling (due to weight). However, adequate strength and stiffness are needed for hydrokinetic and can alone is implemented by the utility of greater enforcement materials so as composite materials, beginning with a design which

* Corresponding author at: Laboratory for Renewable Energy and Dynamic Systems, FSAC - UH2C, Morocco.
E-mail address: mourad.nachtane@ensta-bretagne.org (M. Nachtane).

https://doi.org/10.1016/j.egyr.2018.01.002

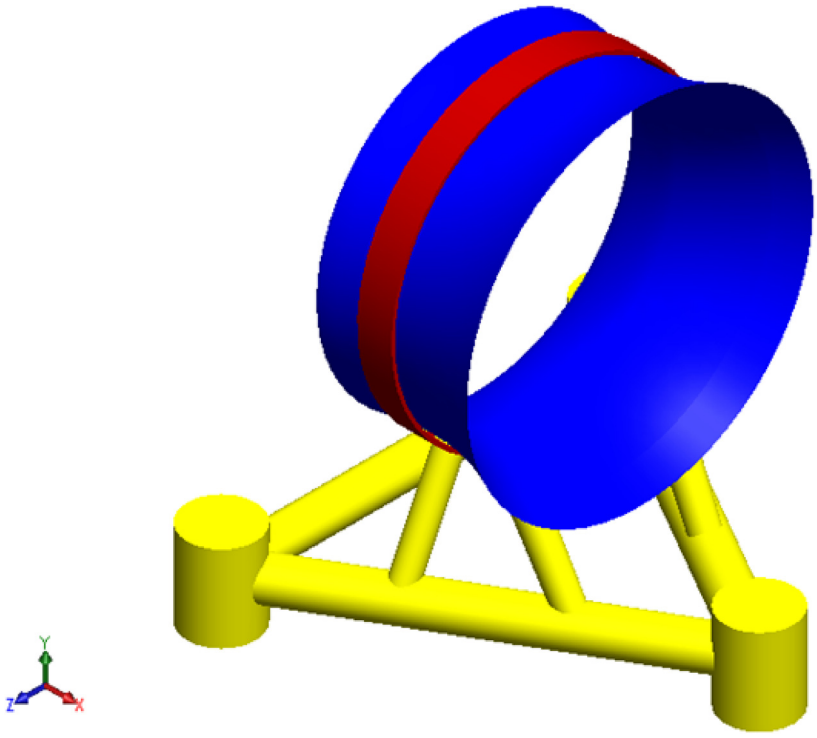

Fig. 1. 3D nozzle of the marine current turbine.

offers an accommodation between efficiency, endurance, weight, and cost.

This research presents a finite element analysis of the mechanical response of composite material applied to renewable marine energy. In order to meet the needs of the manufacturers of tidal current turbines, which is generally linked to a problem of mass gain, composite materials present a considerable asset on account of their excellent mass/rigidity relations. A structural design of ducted tidal current turbines using composite materials has therefore been examined. The duct of the tidal current turbine is especially confronted by the impacts due to its particular position. The impact damage aspect has also been examined in detail in the present research study.

2. Structure and mechanical properties of composites

2.1. Structure

Fig. 1 present the 3D nozzle of the marine current turbine considered in this investigation. We plotted the hydrodynamic profile using the Heliciel software. This structure is then included in the Abaqus finite element code in order to predict its behavior and mechanical performance.

2.2. Mechanical properties of composites

Ducted tidal turbine are routinely subjected to conditions of fatigue loading, which over time results in structural damage that negatively affects blade durability. Structural materials within a tidal turbine blade are therefore of considerable importance, and design parameters for such materials should be reviewed and optimized to decrease fatigue-related losses in strength and stiffness. The structural integrity of the nozzle depends on the combination of composites used to withstand the loads and the highest quality materials which are required for such marine applications.

The shipbuilding industry is dominated by fiberglass reinforced materials because of their mechanical performance and reasonable cost (Davies and Verbouwe, 2017). However, carbon fibers are more robust and lighter and their fatigue strength is much higher, however, there is very little data to describe their response induces many additional costs in manufacturing (Tarfaoui et al., 2017). In this research, we will use these two composite materials to make a comparison to know which of the two materials meets our expectations and industrial requirements. The structural design requires high material strength, high material stiffness, and low density (Nachtane et al., 2017). The composite mechanical properties for glass–polyester and carbon–epoxy are given in Tables 1 and 2.

Table 1
Properties of glass–polyester (Shah and Tarfaoui, 2014).

Properties	Value
ρ (kg/m^3)	1960
E_1 (GPa)	48, 16
E_2 (GPa) $= E_3$ (GPa)	11, 210
Nu_{12}	0, 270
$Nu_{13} = Nu_{23}$	0, 096
G_{12} (GPa) $= G_{13}$ (GPa)	4, 420
G_{23} (GPa)	9
X_t (GPa)	10, 213
X_c (GPa)	0, 978
Y_t (MPa)	29, 5
Y_c (MPa)	171, 8
S_t (MPa) $= S_c$ (MPa)	35, 3

The composites used are the ones taken directly from a real current turbine. They constitute of a Bi-axial fiber mat of 0.286 mm thickness in a resin matrix. The composite has been prepared using hand layup and cured under vacuum bagging under atmospheric pressure at room temperature. The composite lay-up used is symmetrical stack ply orientations [45/ −45/0/90/90/0/ −45/45].

3. Numerical model

The marine current turbine is the mechanical device that captures the kinetic energy of marine current to generate electrical

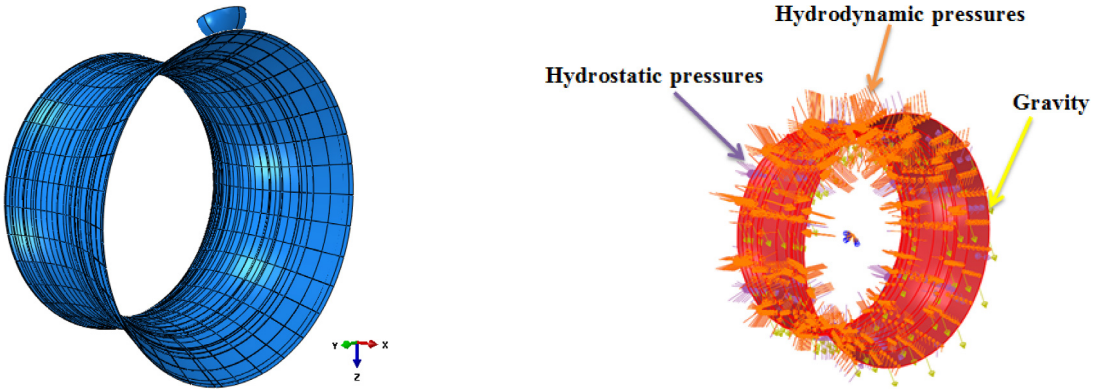

(a) Geometry of model.

(b) Hydrostatic and hydrodynamic conditions.

Fig. 2. Numerical of full model, impactor and nozzle, for impact test and boundary conditions.

Table 2
Properties of carbon–epoxy (Smojver and Soric, 2002).

Properties	Value
ρ (kg/m3)	1600
E_A (GPa)	227
E_T (MPa)	15, 5
E_m (GPa)	3, 46
Nu_A	0, 41
Nu_m	0, 35
G_A (GPa	23, 2
G_T (GPa)	5, 4
Xt (GPa)	1, 5
Xc (GPa)	1, 5
Yt (MPa)	40
Yc (MPa)	246
S_{12} (MPa) = S_{23} (MPa) = S_{13} (MPa)	105

power. One way to increase the efficiency of the tidal turbines is to install augmentation channels (ACHs) to accelerate flow speed. With regard to this augmentation device, different terms such as duct, shroud, wind-lens, nozzle, concentrator, diffuser, or ACH are used synonymously. Ducted turbines are not subjected to the Betz limit. For ducted turbines, the theoretical limit depends on the pressure difference between duct inlet and outlet and the volumetric flow through the duct. These factors depend on the shape of the duct and the ratio of duct area to turbine area.

The addition of a duct could significantly improve the total output power. The duct section induces a circulation which accelerates the water flow into the rotor increasing the available power. The duct however uses a significant part of the cross-section area and in order to be of advantage, the power output has to be superior to the one of a bare rotor using the same overall cross-section area. A panel method program coupled with the blade element momentum theory (BEM) was used to design a bare tidal turbine which reaches 88% of the Betz limit. The addition of a duct for a same overall cross-section area has been investigated.

Numerical modeling plays a very important role in analyzing the behavior of structures subjected to fast loading (Tarfaoui et al., 2009). This analysis, which is based on the resolution of the dynamic equilibrium equation and the energy conservation equation with the boundary conditions imposed on the structure, requires the use of the mechanical behavior of the material involved. This level, to introduce laws that describe the breakdown of composite materials, the Abaqus code offers the user the possibility of using pre-programmed constitutive models such as VUMAT (criterion of Hashin 3D) (Tarfaoui et al., 2008).

In this section, the numerical investigation of damage in nozzle structures can be performed using finite element analysis implemented in commercial code Abaqus. It should be noted that the damage is examined by Hashin's criteria to evaluate the fiber and matrix damage initiation and propagation. The full model shows the turbine part and the impactor region used for simulation and presented in Fig. 2.

The impactor has a hemispherical shape with 12 kg of mass and 3 m/s of velocity.

Hydrodynamic loads are those loads that result from water flowing against and around our nozzle system. Using Blade Element Momentum (BEM) theory to predict their hydrodynamic performances. The ABAQUS DLOAD user define function has been used to implement our interpolation procedure in order to use the hydrodynamic pressures computed with the panel method code as boundary conditions for the finite element analysis.

The meshes of the nozzle for the calculation of the hydrodynamic performances and for the calculation of structure meet different criteria. For hydrodynamic calculation, the nozzle is represented by a surface mesh, composed of very elongated quadrangular meshes in the direction of the flow. This mesh is refined near the leading edge to correctly describe the flow around the nozzle. For the calculation of structure, the nozzle is represented by a mesh composed of shell or volume elements. The structure mesh must make it possible to describe the deformations of the nozzle. In these two cases, the surface of the mesh is composed of quadrangular facets.

The pressure at any depth due to hydrostatic pressures is found using the equation for hydrostatic pressure:

$$P = \rho\, g\, h$$

P = pressure in fluid (N/m^2)
ρ = density of liquid (kg/m^3)
g = acceleration of gravity (9.81 m/s^2)
h = height of fluid column, or depth in the fluid at which the pressure is measured (m).

3.1. Constitutive progressive degradation of composite material

3.1.1. Damaged material response

In this part, we discuss the model of the progressive damage adopted in the simulations by explaining the equation of the different modes of failure. Composite damage takes place in two phases: the initiation of damage and the evolution of the damage. We adopt here the model proposed by Matzenmiller et al. (1995) in order to

Table 3
Hashin failure criteria (Hashin, 1980).

Fiber Tensile Failure ($\sigma_{11} \geq 0$)	$f_{ft} = \left(\frac{\sigma_{11}}{X_t}\right)^2 \geq 1$
Fiber Compression Failure ($\sigma_{11} < 0$)	$f_{fc} = \left(\frac{\sigma_{11}}{X_c}\right)^2 \geq 1$
Matrix Tensile Failure ($\sigma_{22} + \sigma_{33}) \geq 0$	$f_{mt} = \frac{(\sigma_{22}+\sigma_{33})^2}{Y_t^2} + \frac{\sigma_{23}^2 - \sigma_{22}\sigma_{33}}{S_{23}^2} + \left(\frac{\sigma_{12}}{S_{12}}\right)^2 + \left(\frac{\sigma_{13}}{S_{13}}\right)^2 \geq 1$
Matrix Compression Failure ($\sigma_{22} + \sigma_{33}) < 0$	$f_{mc} = \frac{1}{Y_c}\left(\left(\frac{Y_c}{2S_{23}}\right)^2 - 1\right)(\sigma_{22} + \sigma_{33}) + \frac{(\sigma_{22}+\sigma_{33})^2}{4S_{23}^2} + \frac{\sigma_{23}^2 - \sigma_{22}\sigma_{33}}{S_{23}^2} + \left(\frac{\sigma_{12}}{S_{12}}\right)^2 + \left(\frac{\sigma_{13}}{S_{13}}\right)^2 \geq 1$

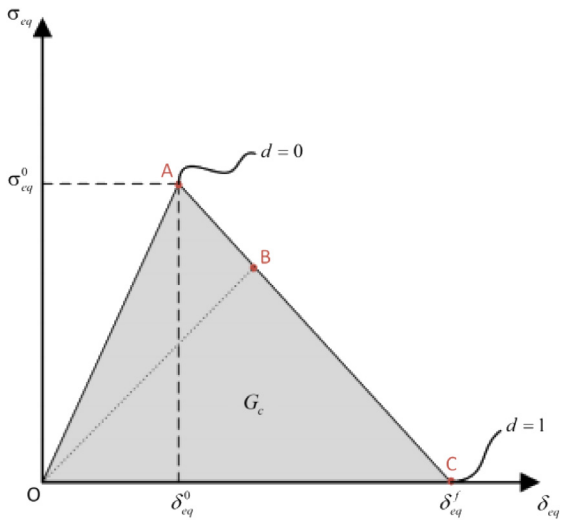

Fig. 3. Constitutive response of interlaminar damage model (Nachtane et al., 2017).

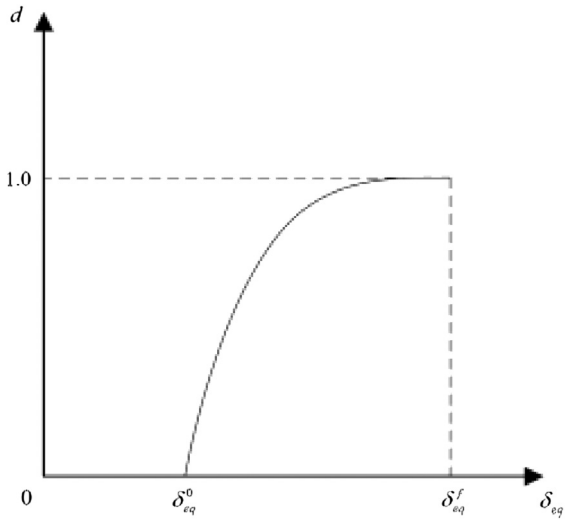

Fig. 4. Saturation type evolution behavior of matrix damage variable d (Nachtane et al., 2017).

calculate the degradation of the coefficients of the stiffness matrix. In this model, the constitutive relations that give the relationship between the effective stress ($\hat{\sigma}$) and the nominal stress (σ) for the damaged composite laminates can be defined as:

$$\hat{\sigma} = d \cdot \sigma \tag{1}$$

where d is the damage operator.

Thus stress with presence of the damages is given as:

$$\sigma_{i,j} = C_{i,j}(d) \cdot \varepsilon_{i,j} \tag{2}$$

where C represents the undamaged orthotropic stiffness matrix. This matrix takes the following form:

$$C = \begin{bmatrix} C_{11} & C_{12} & C_{13} & 0 & 0 & 0 \\ C_{12} & C_{22} & C_{23} & 0 & 0 & 0 \\ C_{13} & C_{23} & C_{33} & 0 & 0 & 0 \\ 0 & 0 & 0 & C_{44} & 0 & 0 \\ 0 & 0 & 0 & 0 & C_{55} & 0 \\ 0 & 0 & 0 & 0 & 0 & C_{66} \end{bmatrix}. \tag{3}$$

Then the damage stiffness matrix is as given in Box I.

$$\begin{aligned} dC_{11} &= \left(1 - d_f\right) E_1 (1 - v_{23}^2) \Gamma, & dC_{22} &= \left(1 - d_f\right)(1 - d_m) E_2 (1 - v_{13}^2) \Gamma \\ dC_{33} &= \left(1 - d_f\right)(1 - d_m) E_3 (1 - v_{21}^2) \Gamma, & dC_{12} &= \left(1 - d_f\right)(1 - d_m) E_1 (v_{21} - v_{31} v_{23}) \Gamma \\ dC_{23} &= \left(1 - d_f\right)(1 - d_m) E_2 (v_{32} - v_{12} v_{31}) \Gamma, & dC_{31} &= \left(1 - d_f\right)(1 - d_m) E_1 (v_{31} - v_{21} v_{32}) \Gamma \\ dC_{44} &= \left(1 - d_f\right)(1 - d_{mt} s_{mt}) E_1 (1 - d_{mc} s_{mc}) G_{12}, & dC_{55} &= \left(1 - d_f\right)(1 - d_{mt} s_{mt}) E_1 (1 - d_{mc} s_{mc}) G_{23} \\ dC_{66} &= \left(1 - d_f\right)(1 - d_{mt} s_{mt}) E_1 (1 - d_{mc} s_{mc}) G_{31}, \end{aligned} \tag{4}$$

where the damage variables and Γ are given by Eq. (5) :

$$\begin{aligned} d_f &= 1 - \left(1 - d_{ft}\right)\left(1 - d_{fc}\right) \\ d_m &= 1 - (1 - d_{mt})(1 - d_{mc}) \\ \Gamma &= 1/(1 - v_{12}^2 - v_{23}^2 - v_{13}^2 - 2 v_{12} v_{23} v_{13}) \end{aligned} \tag{5}$$

where d_f, d_m and d_s is the damage variables for the fiber, matrix and shear failure mode respectively.

Box I.

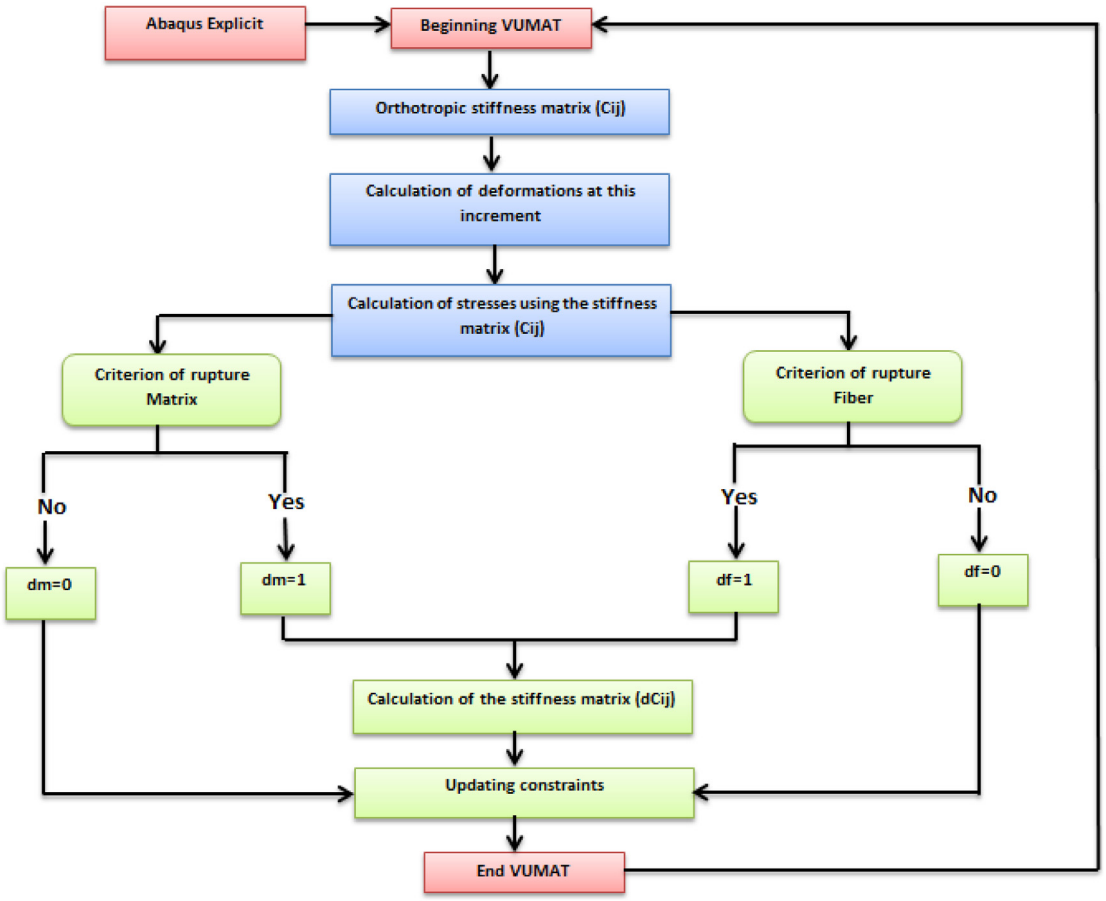

Fig. 5. Numerical implementation of the damage model with VUMAT under Abaqus.

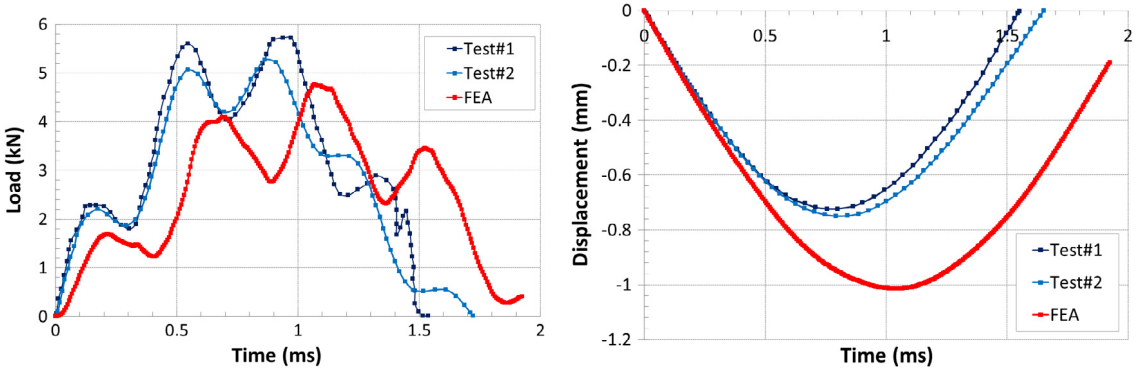

Fig. 6. Confrontation test/FEA, $V = 2.55$ m/s (Tarfaoui et al., 2008).

3.1.2. Intralaminar failure based continuum damage mechanics

Among the fiber and matrix damage that can take place within a lamina. However, in many damage investigations, only the intralaminar damage mechanism is modeled and the interlaminar damage mechanism is ignored or vice-versa without adequate justification. In this purpose, a user material VUMAT subroutine was compiled in FORTRAN code and implemented by the finite element explicit Abaqus software to characterize the intralaminar damage. To simulate the evolution of the damage, modeling must take into account the various forms of damage occurring at the impact tests. It is not necessary that the numerical model take account all the physical phenomena observed if their presence does not affect in a relevant way the current turbine behavior. This choice was dictated by the infiltration of water in the presence of this type of damage and which can lead to the rapid degradation of the material due to aging effect. For that, the Hashin criteria (Garnier, 2011) were used.

3.1.3. Damage initiation criteria

Damage modeling in laminate composites can be studied by a stress or strain-based failure criteria approach or following damage mechanics concepts. Hashin's has proposed four failure criteria for composites namely: fiber damage in tension and compression and matrix tensile and compressive failure. These criteria have been widely applied to predict the initiation of damage in unidirectional composites (Garnier, 2011; Hashin, 1980). In the present study, these criteria were proposed for both fibers and matrix, and listed in Table 3.

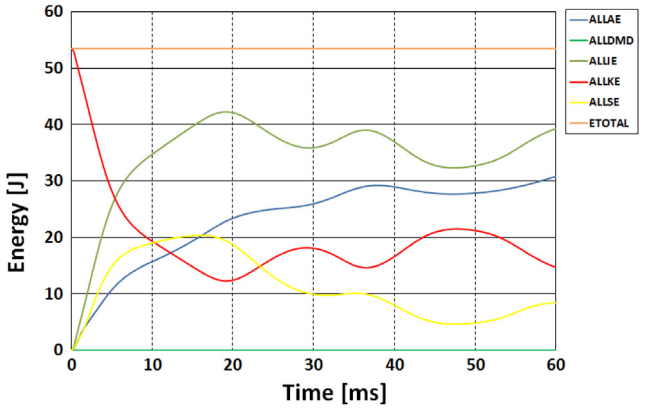

Fig. 7. Evolution of impact energies during the period test ($m = 12$ kg, $V = 3$ m/s).

Hashin's criteria are very popular in composite structural applications due to their simplicity of concept and ease of use; they do not always fit experimental results well. The main disadvantage of these criteria is that they combine fundamentally different fracture mechanisms of the UD layer together. In addition, these interactive criteria are unable to directly determine the initial failure mode, which is necessary for progressive failure analysis of composite structures.

3.1.4. Damage evolution criterion

The damage evolution phenomena is an irreversible process, the reduction in stiffness material properties is controlled by damage variables corresponding damage modes despite Satisfied the initiation of the failure modes in the composite materials, the material's stiffness continues to degrade with increasing the load (El Moumen et al., 2017). Based on the relationship between the effective stress and displacement, damage evolution can be constituted. Therefore, damage variables for each mode in the fibers and matrices are expressed in the form of the displacement:

$$d_i = \frac{\delta^f_{i,eq}(\delta_{i,eq} - \delta^0_{i,eq})}{\delta_{i,eq}(\delta^f_{i,eq} - \delta^0_{i,eq})}, \quad \delta^0_{i,eq} \leq \delta_{i,eq} \leq \delta^f_{i,eq} \tag{6}$$

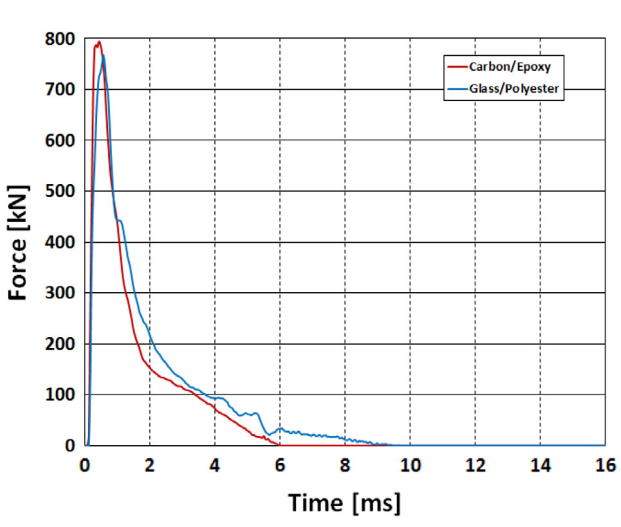

Contact Force

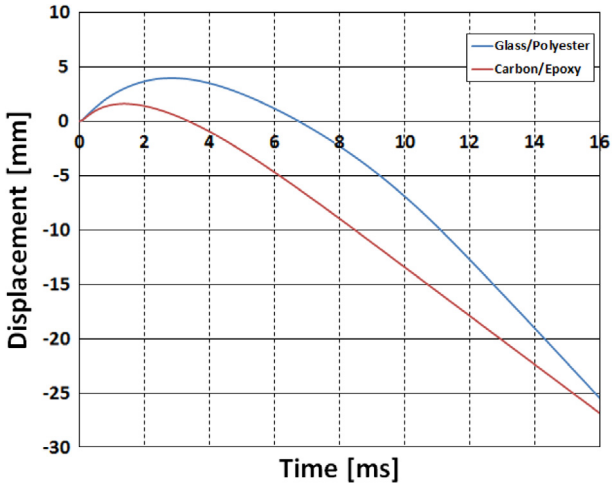

Displacement

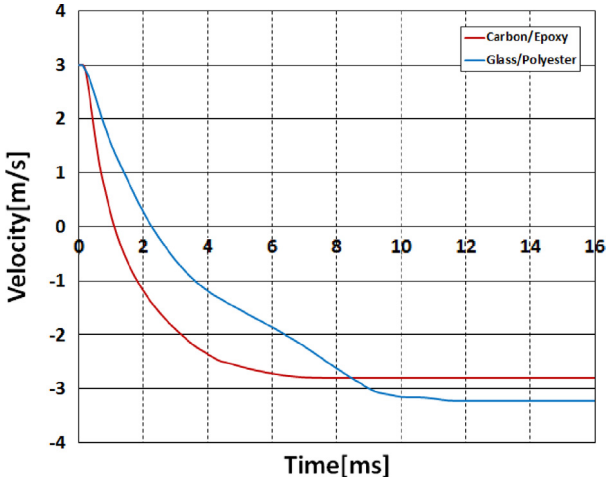

Velocity

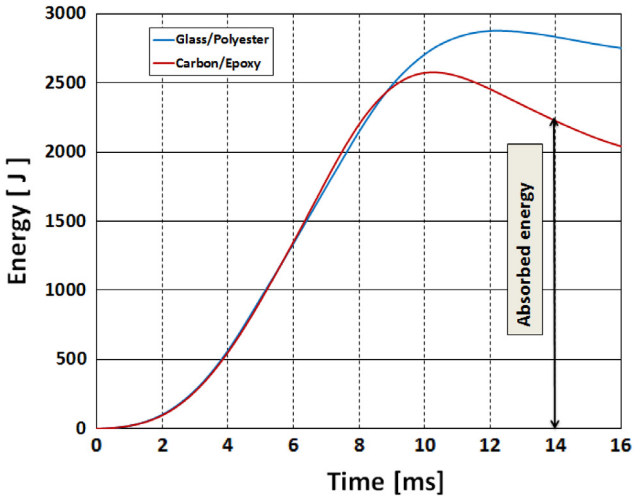

Absorption energy

Fig. 8. Results of numerical simulation ($m = 12$ kg, 3=m/s).

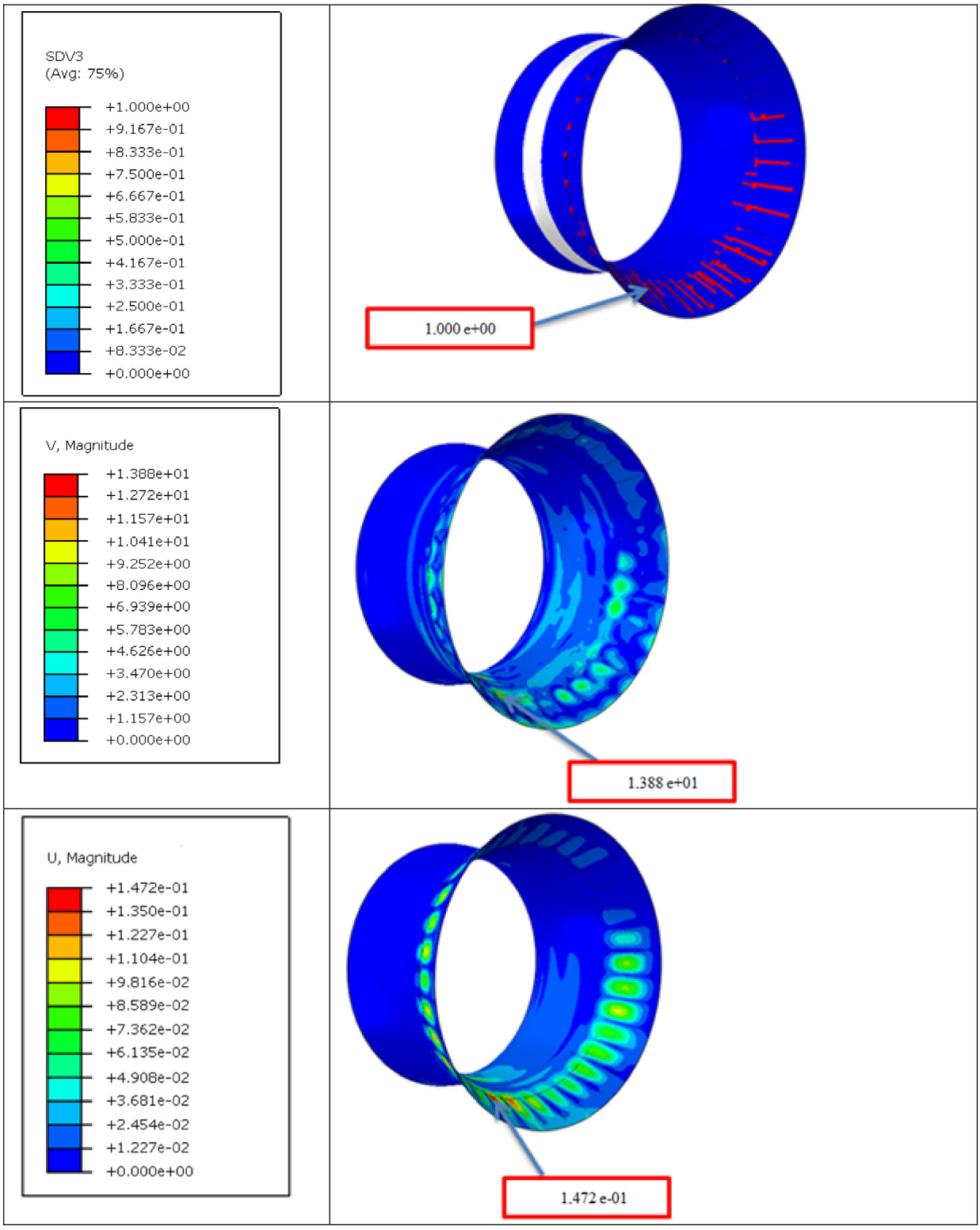

Fig. 9. Damage of the nozzle under hydrodynamics, hydrostatics loads and impact for Glass/polyester composite.

where, $(\delta^0_{\acute{e}q})$ and $(\delta^f_{\acute{e}q})$ are the equivalent displacements at the initiation point of damage and at the completely propagated damage state, respectively, in Eq. (6) $d_m = 0$ corresponds to point A and $d = 1$ corresponds to point C in Fig. 3. The saturation type evolution of damage variable with d respect to equivalent displacement δ_{eq} is illustrated in Fig. 4.

For more illustration, the algorithm of the proposed model is illustrated in Fig. 5.

4. Results and discussion

In this section, we present the results of the FE simulation by analyzing the dynamic response of the nozzle subjected to impact

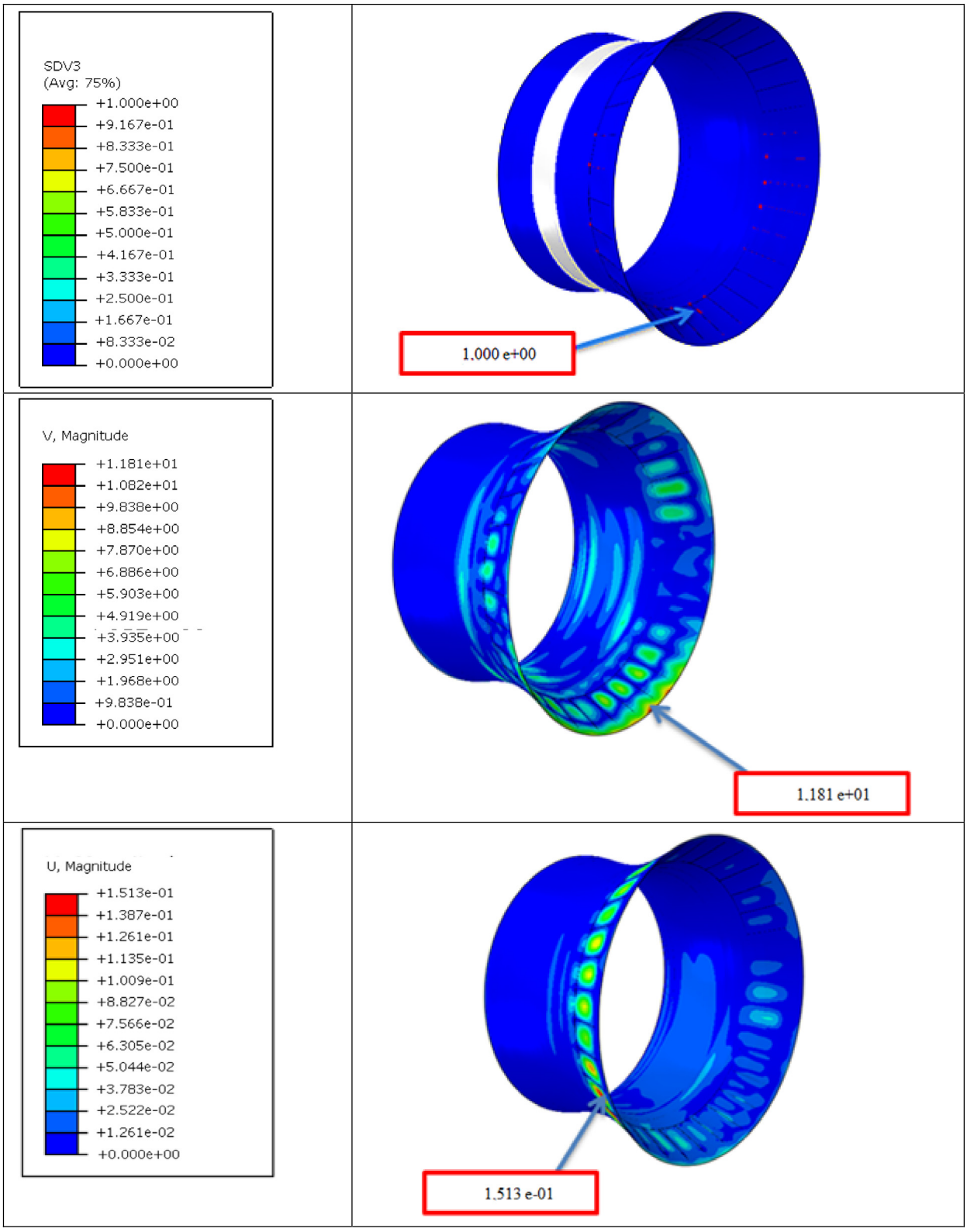

Fig. 10. Damage of the nozzle under hydrodynamics, hydrostatics loads and impact for Carbon/Epoxy composite.

tests more the hydrodynamic pressure calculated during the rotor design and the hydrostatic pressure related to the depth of the site and to the circulation of the fluid at a speed of 3 m/s.

We have interested in this part to the validation of the created model, validation of the VUMAT subroutine and the behavior laws of the ply implemented in the VUMAT for different velocities of impact. For that purpose, experimental tests (Tarfaoui et al., 2008) were conducted on the cylindrical structures and the obtained results are compared with those of numerical model with VUMAT. For the case of impact with damaged structures: 5.202 J (V = 2.55 m/s), the comparison is given in Fig. 6. The impact curves of the impactor have a temporal evolution similar to that of the

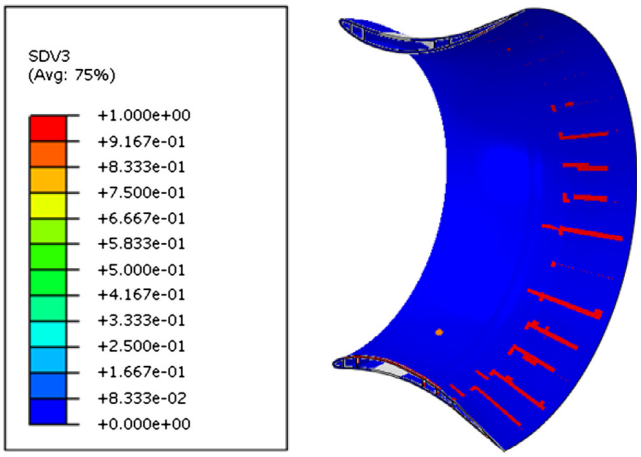

Fig. 11. Failure criterion of matrix in tension (SDV3).

experimental values but overestimate the value of the displacements. In general, the impact model presents a reasonable fit with the experimental measurements.

4.1. Energy conservation

The examination of the variation of the energy makes it possible to prove the theory of the conservation of the energy of the system. Fig. 7 shows the variation of the energies for an impact velocity of 3 m/s. We perceive that the total energy (ETOTAL) is constant throughout the calculation and corresponds to the desired energy impact. In addition, the summation of the kinetic energy (ALLKE) and the internal energy (ALLIE) corresponds to the total energy. Consequently, energy conservation during the impact test is obtained. On the other hand, in order to validate the hypothesis of energy conservation, we remark that the internal energy of the structure is the sum of the damage of the energy of deformation and the dissipation of energy.

4.2. Damaged structures

The Fig. 8 shows the results of numerical simulation for both materials with velocity of 3 m/s under hydrodynamic and hydrostatic loadings. Carbon/epoxy durability is perceptible compared to glass/polyester and as expected, the impact force increases during the time producing more damage with a consequent change in displacement/speed. The maximum force for each type of material is: 800 kN for carbon/epoxy and 760 kN for glass/polyester. Initially, the curve was linear and then became non-linear after the peak force due to initiation of damage. On the other hand, the energy absorbed is the energy absorbed by the structures by the formation of damage and the friction between the impacted specimens and the impactor. It is concluded that the energy absorption capacity of the carbon/epoxy is lower than the glass/polyester.

A finite element (FE) investigation into the impact performance at low speed of nozzle was considered without penetration of the target by the striking element using the most advanced modeling techniques currently available Abaqus/explicit. For this type of impact, the main damage modes were: matrix cracking; fiber failure rarely occurred. Impact damage begins with localized cracking matrix which acts as an initiation point for delamination propagation. Two types of a crack matrix can be observed as shown in Figs. 9 and 10: vertical and oblique cracks. Vertical cracks are introduced by the bending of deformations due to tensile stresses and are generally located in the bottom of the folds. Slant fissure is formed on the top of the transverse shear stresses due to the flexural deformation of the component. These cracks are usually located at the top or middle of pleats. Even if the crack matrix does not significantly reduce the laminated properties, they work as delamination initiation point.

During the impact, the displacement of the impactor and the contact force are measured. The results obtained show that the maximum force, as well as the maximum displacement, evolves linearly and depend on composite types. The maximum displacement is the most influential parameter for the creation of ruptures by buckling.

The impact was conducted on the trailing edge because it is the critical sensitive part. We remark that the damaged areas are similar for both materials, however, a comparison of the results of Hashin criteria of the two materials used in the simulations, explains that it is evident that carbon–epoxy, with $m = 176{,}352$ kg, is higher resistant and provides for lighter weight than glass–polyester, with $m = 216{,}031{,}1$ kg. It can be seen that the displacement and velocity for Carbon/Epoxy is less than Glass/polyester (see Figs. 9 and 10).

The composite material damage is a cumulative of the microscopic defects in both the fiber and the matrix and other types of failure, the initiation and developments of the micro-cracks with different scale size internal and external of the structure considered the main factor in the fracture mechanism. In this simulation results we looks non-symmetric because the nozzle are subjected to critical loads due to the high density of seawater and the accidental impacts in what they operate.

The impact was performed on the trailing edge because it is the most sensitive part. One can see that there is an appearance of damage. Hashin criterion for matrix in tension (HSNMTCRT) has been reached for some layers. In the other hand, Hashin criterion for matrix in compression (HSNMCCRT), for fiber in tension (HSNFTCRT) and for fiber in compression (HSNFCCRT) is not checked.

Fig. 11 show contour plots of impacted nozzle and the evolution of predicted damage areas. Damage is widespread towards the leading edge of structures in which SDV3 $=$ 1, this means the element is damaged. The damage is visible and concentrated in the edge surface of the nozzle structure. In this zone, striker developed stress concentrations causing more damage in the structure.

5. Conclusion

The study of the damage phenomena of the marine current turbine under different loading scenarios including impact with the presence of hydrostatic and hydrodynamic loads has all its interest for the designer. Indeed, even a small damage can have a considerable effect on the durability of the structure. In this investigation, the numerical simulation of damage progressive was conducted for predicting failure modes and identifies the sensitive zones on tidal turbine as well as to determine the effect of the material used for the construction, the improvement of the structure of nozzle and the reduction of damage. Generally, the damage begins at microscopic scale with firstly matrix cracking, fibers/matrix breaking, and delamination and finally ends with fibers failure. The principle conclusions are: Each of the composite materials used in the simulations has its qualities and limits, composites with fiberglass are economically very attractive for medium-sized wind turbine blades, but composites with carbon fibers offer excellent properties and good resistance to fracture under quasi-static and dynamic loadings.

References

Boisseau, A., Davies, P., Thiebaud, F., 2012. Sea water ageing of composites for ocean energy conversion systems: influence of glass fibre type on static behaviour. Appl. Compos. Mater. 19 (3–4), 459–473.

Boisseau, A., Davies, P., Thiebaud, F., 2013. Fatigue behaviour of glass fibre reinforced composites for ocean energy conversion systems. Appl. Compos. Mater. 20 (2), 145–155.

Davies, P., Lemoine, L., 1992, December. Nautical applications of composite materials. In: Proc 3rd IFREMER Conference.

Davies, P., Verbouwe, W., 2017. Evaluation of basalt fibre composites for marine applications. Appl. Compos. Mater. 1–10.

El Moumen, A., Tarfaoui, M., Hassoon, O., Lafdi, K., Benyahia, H., Nachtane, M., 2017. Experimental study and numerical modelling of low velocity impact on laminated composite reinforced with thin film made of carbon nanotubes. Appl. Compos. Mater. 1–12.

Garnier, C., 2011. Etude du comportement dynamique des structures composites réalisées par LRI: application à l'impact et à la fatigue. Thèse de doctorat.

Hashin, Z., 1980. Failure criteria for unidirectional fiber composites. J. Appl. Mech. 47, 329–334.

Matzenmiller, A., Lubliner, J., Taylor, RL., 1995. A constitutive model for anisotropic damage in fiber-composites. Mech. Mater. 20, 125–152.

Mourad, N., Mostapha, T., Dennoun, S., 2018. Promotion of renewable marines energies in Morocco: Perspectives and strategies. Int. J. Energy Power Eng. 5 (1).

Nachtane, M., Tarfaoui, M., El Moumen, A., Saifaoui, D., 2016. Numerical investigation of damage progressive in composite tidal turbine for renewable marine energy. In: 2016 International Renewable and Sustainable Energy Conference. IRSEC, IEEE, p. 559-563.

Nachtane, M., Tarfaoui, M., El Moumen, A., Saifaoui, D., 2017. Damage prediction of horizontal axis marine current turbines under hydrodynamic, hydrostatic and impacts loads. Compos. Struct. 170, 146–157.

Nachtane, M., Tarfaoui, M., Saifaoui, D., 2017. Matériaux composites pour les énergies marines renouvelables. Éditions universitaires européennes, ISBN: 620226 1579.

Smith, C.S., 1990. Design of Marine Structures in Composite Materials. Elsevier, London.

Shah, O.R., Tarfaoui, M., 2014. Effect of damage progression on the heat generation and final failure of a polyester–glass fiber composite under tension–tension cyclic loading. Composites B 62, 121–125.

Smojver, I., Soric, J., 2002. Impact damage analysis of layered composite plates, in: Proceedings of DESIGN, The 7th International Design Conference, DS 30, Dubrovnik.

Tarfaoui, M., Gning, P.B., Collombet, F., 2009. Damage modelling of impacted tubular structures by using material property degradation approach. In: Damage and Fracture Mechanics. Springer, Netherlands, pp. 227–235.

Tarfaoui, M., Gning, P.B., Hamitouche, L., 2008. Dynamic response and damage modeling of glass/epoxy tubular structures: Numerical investigation. Composites A 39 (1), 1–12.

Tarfaoui, M., Nachtane, M., Khadimallah, H., Saifaoui, D., 2017. Simulation of mechanical behavior and damage of a large composite wind turbine blade under critical loads. Appl. Compos. Mater. 1–18.